MINIMIZATION THE DEFLECTION AND COST OF REINFORCEMENT FRAME USING DOE

Sabah Khammass Hussein*

Assist. Prof. Dr., Technical College, Baghdad, Iraq.

Abstract: The stiffening of a rectangular frame is taking place by using bars. Those bars are distributed longitudinally, transversely, inclined and mixed shape. The theoretical deflection of frame free edge is calculated and compared with the (FEM) using MATLAB and ANSYS software programs. A good agreement is found from the (FEM) model as compared with the theoretical and ANSYS results. Different bar distributions gave a different torsional resistance and deflection. A higher torsional resistance is found in the transverse and cross shape of bar distributions. Minitab program is used to analyze the results and minimize the deflection and cost by (DOE). In which, the effect of input factors and their interactions has been studied. The main effect on the deflection and cost has been observed in the inclined bars. A higher reduction in the deflection and cost has been observed in the existence of longitudinal and transverse bars, respectively.

Keywords: *Frame deflection, frame torsional resistance, frame stiffening, DOE.*

تقليل انحراف وكلفة الهياكل المقواة بأستخدام طريقة تصميم التجارب

الخلاصة: هذه الوثيقة هي قالب حي. المكونات المختلفة من البحث [العنوان، النص، الحاشيات، إلخ] قد تم تعريفها بالفعل على الورقة النمطية تتم تقوية الهيكل المستطيل بأستخدام قضبان. وزعت هذه القضبان بشكل طولي، عرضي، مائل ومدموج. الانحراف النظري لحافة الهيكل الحرة حُسِب وقُورن مع طريقة العناصر المحددة باستخدام برنامجي ال (MATLAB) و ال(ANSYS). لاحظنا توافق جيد لنموذج طريقة العناصر المحددة مقارنة مع نتائج الجزء النظري وال(ANSYS). التوزيعات المختلفة للقضيب اعطت اختلاف بمقاومة الألتواء والانحراف. اعلى مقاومة التواء وجدت في توزيع القضبان بشكل عرضي ومتقاطع. استخدم برنامج ال(Minitab) لتحليل النتائج وتقليل الانحراف والكلفة بطريقة ال (DOE). حيث دُرس تأثير العوامل الداخلة وتداخلاتها. لوحظ التأثير الرئيسي على الانحراف والكلفة في القضبان المائلة. اعلى نسبة تخفيض في الانحراف والكلفة لوحظت بوجود القضبان بالشكل الطولي والعرضي على التوالي.

1. Introduction

Torsional loading is the application of a force that tends to cause the member to twist about its structural axis. This type of loading is associated with axles, spindles and other rotating frame members. The principal deflection caused by torsion is measured by the angle of twist, or by the vertical movement of one corner of the frame or base [1 & 2]. In order to increase the frame stiffener, transverse, longitudinal or inclined stiffeners can be weld in this frame. This will reduce the vertical deflection [3]. Two methods are used for the optimum design and comparison of the two methods and uniaxial compressed plates stiffened by ribs of

_____

* sabah.kh1974@yahoo.com

various shapes.Both methods consider the effect of initial imperfection and residual welding stresses, but their empirical formulae are different. The elastic secondary deflection due to compression and lateral pressure is calculated using the Paik's solution and besides this deflection, some more deformations are caused by lateral pressure and the shrinkage of longitudinal welds [4]. The beam design method for semi-rigid composite frames with vertical loading at the serviceability limit state has been simplified. Equations were developed to determine the deflections of the composite beam allowing for both joint flexibility and beam sectional properties, along with a formula for the connection secant stiffness. The equations were validated by the experimental results for two semi-rigid composite frames. The equations agree well with the experimental data because they take into account the actual beam-to-column [5]. The deflection of thin rectangular plates loaded by point loads and stiffened by elastic beams is determined using an infinite series approach. Both bending and torsional beam stiffness are included in the formulations. Solutions are obtained, and are results presented for a variety of plate aspect ratios and beam stiffness values. Comparisons of the results obtained with available solutions demonstrate a good agreement, and parametric studies show the utility of this approach for various ratios of beam stiffness (bending and torsional) to plate stiffness [6].

2. Finite Element Method:

A frame structure is made from many members connected together. It may be planer or spatial geometry. Each beam members in planer frame structure generally subject to both bending and axial loading.
The static analysis of a beam or a frame is to solve the following matrix [7]:

$$[k]\{d\} = \{F\} \tag{1}$$

Where:

[k]: system stiffness matrix.

{d}: system displacement vector.

{F}: system force vector.

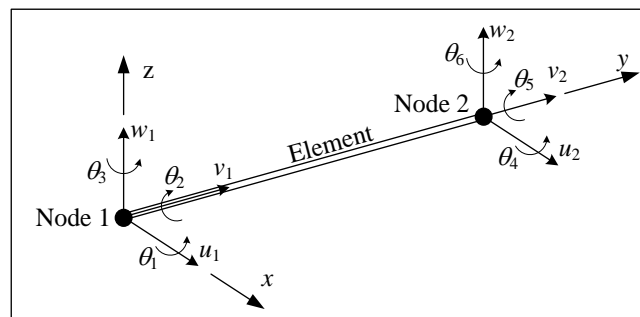To solve the above equation (1), assume the frame element is as shown in figure (1).

Figure (1) Spatial frame element [7].

The three dimension element consists of two nodes (1, 2). The corresponding element degree of freedom is:

$$\{d^e\} = \{u_1 \ v_1 \ w_1 \ \theta_1 \ \theta_2 \ \theta_3 \ u_2 \ v_2 \ w_2 \ \theta_4 \ \theta_5 \ \theta_6\}^T \tag{2}$$

Those variables represent the degree of freedom for each node; where:

u_1, u_2: the deformation in the x-direction for nodes (1&2), respectively.

v_1, v_2: the deformation in the y-direction for nodes (1&2), respectively.

w_1, w_2: the deformation in the z-direction for nodes (1&2), respectively.

θ_1, θ_4: the slopes associated with bending moments about x-axis for nodes (1&2), respectively.

θ_2, θ_5: the rotational degree of freedom associated with twisting moments for nodes (1&2), respectively.

θ_3, θ_6: the slopes associated with bending moments about z-axis for nodes (1&2), respectively.

The element stiffness in a local axis is as seen in figure (1) and has the following matrix [7, 8 & 9]:

$$[k^e] = \begin{bmatrix} k^e_{11} & k^e_{12} \\ k^e_{21} & k^e_{22} \end{bmatrix} \tag{3}$$

Where:

$$[k^e_{11}] = \begin{bmatrix} a_1 & 0 & 0 & 0 & 0 & 0 \\ 0 & b_1 & 0 & 0 & 0 & b_2 \\ 0 & 0 & c_1 & 0 & c_2 & 0 \\ 0 & 0 & 0 & a_2 & 0 & 0 \\ 0 & 0 & -c_2 & 0 & -2c_3 & 0 \\ 0 & b_2 & 0 & 0 & 0 & -2b_3 \end{bmatrix} ; \quad [k^e_{12}] = [k^e_{21}]^T =$$

$$\begin{bmatrix} -a_1 & 0 & 0 & 0 & 0 & 0 \\ 0 & -b_1 & 0 & 0 & 0 & b_2 \\ 0 & 0 & -c_1 & 0 & -c_2 & 0 \\ 0 & 0 & 0 & -a_2 & 0 & 0 \\ 0 & 0 & c_2 & 0 & c_3 & 0 \\ 0 & -b_2 & 0 & 0 & 0 & b_3 \end{bmatrix} ;$$

$$[k^e_{22}] = \begin{bmatrix} a_1 & 0 & 0 & 0 & 0 & 0 \\ 0 & b_1 & 0 & 0 & 0 & -b_2 \\ 0 & 0 & c_1 & 0 & c_2 & 0 \\ 0 & 0 & 0 & a_2 & 0 & 0 \\ 0 & 0 & c_2 & 0 & 2c_3 & 0 \\ 0 & -b_2 & 0 & 0 & 0 & 2b_3 \end{bmatrix} \tag{4}$$

Where:

$a_1 = \dfrac{EA}{L}$; $a_2 = \dfrac{GJ}{L}$; $b_1 = \dfrac{12EI_x}{L^3}$; $b_2 = \dfrac{6EI_x}{L^2}$; $b_3 = \dfrac{2EI_x}{L^2}$; $c_1 = \dfrac{12EI_z}{L^3}$; $c_2 = \dfrac{6EI_z}{L^2}$; $c_3 = \dfrac{2EI_z}{L^2}$

In general, a beam member is inclined to the global coordinate system, as shown figure (2). In this case (frame), the element stiffness matrix requires the planers transformation. Figure (3) shows a two vcoordinate system: local and global system.
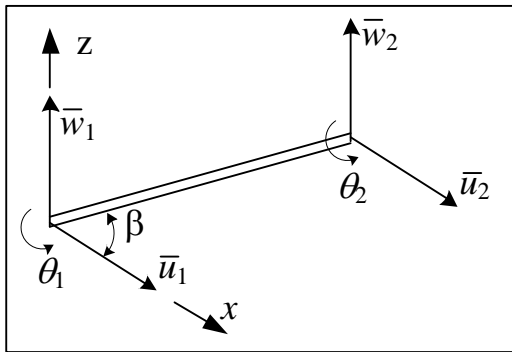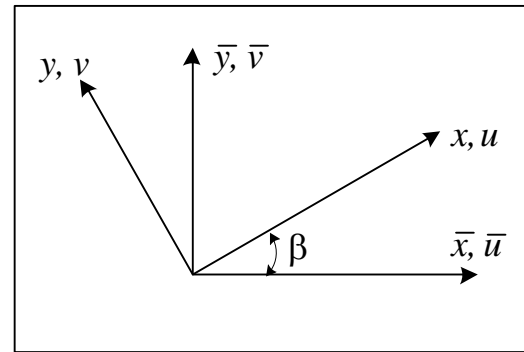
Figure (2) Inclined frame element.

Figure (3) Coordinate transformation.

The global system is denoted by a superimposed bar on both coordinate axes and displacements. The relation between the local and global displacement is:

$$\begin{Bmatrix} u_1 \\ v_1 \\ w_1 \\ \theta_1 \\ \theta_2 \\ \theta_3 \\ u_2 \\ v_2 \\ w_2 \\ \theta_4 \\ \theta_5 \\ \theta_6 \end{Bmatrix} = \begin{bmatrix} c & s & 0 & 0 & 0 & 0 & 0 & 0 & 0 & 0 & 0 & 0 \\ -c & s & 0 & 0 & 0 & 0 & 0 & 0 & 0 & 0 & 0 & 0 \\ 0 & 0 & 1 & 0 & 0 & 0 & 0 & 0 & 0 & 0 & 0 & 0 \\ 0 & 0 & 0 & 1 & 0 & 0 & 0 & 0 & 0 & 0 & 0 & 0 \\ 0 & 0 & 0 & 0 & 1 & 0 & 0 & 0 & 0 & 0 & 0 & 0 \\ 0 & 0 & 0 & 0 & 0 & c & s & 0 & 0 & 0 & 0 & 0 \\ 0 & 0 & 0 & 0 & 0 & -s & c & 0 & 0 & 0 & 0 & 0 \\ 0 & 0 & 0 & 0 & 0 & 0 & 0 & 1 & 0 & 0 & 0 & 0 \\ 0 & 0 & 0 & 0 & 0 & 0 & 0 & 0 & 1 & 0 & 0 & 0 \\ 0 & 0 & 0 & 0 & 0 & 0 & 0 & 0 & 0 & 1 & 0 & 0 \\ 0 & 0 & 0 & 0 & 0 & 0 & 0 & 0 & 0 & 0 & 1 & 0 \\ 0 & 0 & 0 & 0 & 0 & 0 & 0 & 0 & 0 & 0 & 0 & 1 \end{bmatrix} \begin{Bmatrix} \bar{u}_1 \\ \bar{v}_1 \\ \bar{w}_1 \\ \bar{\theta}_1 \\ \bar{\theta}_2 \\ \bar{\theta}_3 \\ \bar{u}_2 \\ \bar{v}_2 \\ \bar{w}_2 \\ \bar{\theta}_4 \\ \bar{\theta}_5 \\ \bar{\theta}_6 \end{Bmatrix} \quad (5)$$

Where:

$$c=cos\beta \; ; \; s=sin\beta \qquad (6)$$

In a short notation, Eq. (5) can be written as:

$$\{d^e\} = [T]\{\bar{d}_e\} \qquad (7)$$

Where:

$[T]$: transformation matrix.

The stiffness matrix for a planer frame element is expressed in term of the global coordinate system as given below:

$$[\bar{K}^e] = [T]^T[K^e][T] \qquad (8)$$

2.1. Finite Element Program Using MATLAB

A MATLAP program is used to solve the static deflection for all cases osf (3D-frame) [10, 11 & 12]. To explain the program steps, assume the following case, fig. (4). Due to symmetry, only half frame can be used in the finite element program.

Step1: input the element, node, node degrees of freedom and the system degrees of freedom numbers, fig.(5):

A half frame is shown in figure (5) where the element numbers will be (15-element). The length of each element is (20 mm). Each node has (6-degree of freedom); that means the total degree of freedom for each element (have 2-node) will be (12-degree of freedom).
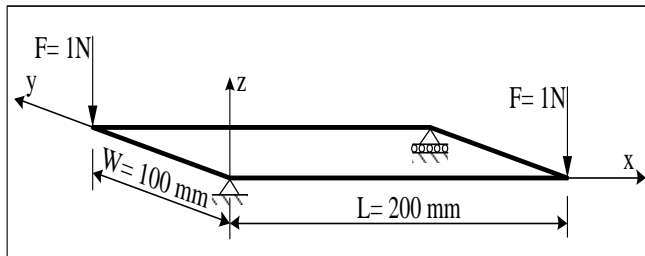

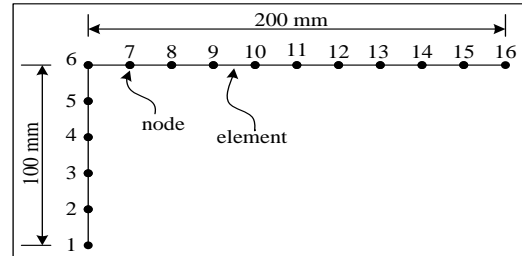Figure (4) Schematic of simply supported
frame at the opposite corner.

Figure (5) Finite elementmodel
of the half frame

Step 2: input the node coordinates:

This step include the input data of node coordinate (x,y,z). The frame is assumed in the (xy-plane).

Step 3: input the boundary conditions:

The boundary conditions are applied at nodes (1&16) as follows:

Node 1: constraint through (x,y and z-axis); that means (u,v and w=0).

Node 16: constraint through (z-axis) only; that means the deflection through the z-axis will be zero (w=0).

Step 4: input the applied force, material and sectional properties:

The (1N) force is applied at node (6) in the negative direction of (z-axis). The input data of material properties (carbon steel) used in this search include the modules of elasticity (E= 200 Gpa.), poison's ratio (v=0.3) and the modulus of rigidity (G=77 Gpa.).

Step 5: system stiffness matrix:

The element stiffness matrix is computed from Eq. (3) and then assembled into system stiffness matrix taking into account the transformation matrix.

Step 6: solution step:

In this step, the solution of matrix system is given.

3. Theoretical Deflection Analysis of Built-up Frame:

In analyzing the resistance and strength of built-up frame against twisting, consider the torque applied as two forces in the form of a couple at each end of the frame. These same forces apply a torque transverse and longitudinal to the frame. This helps to show that the overall resistance against twisting is the sum of resistance of all members, longitudinal as well as transverse. It is usually more convent to express the resulting angular twists in terms of vertical deflection of the frame corner which receives the vertical load [3].

When the vertical force (F) applied at the corner, the frame will deflect vertically to a given distance (Δ). Each longitudinal and transverse member will twist (θ_L & θ_T), respectively, the following relation is found:

$$\Delta= \theta_L\, W = \theta_T\, L \qquad\qquad (9)$$

Then:

$$\theta_L = \frac{\Delta}{W} \quad and \quad \theta_T = \frac{\Delta}{L} \qquad\qquad (10)$$

Where:

Δ: vertical deflection under the applied load (mm).

θ_L: longitudinal twist angle (degree).

θ_T: transverse twist angle (Rad.).

L: length of longitudinal member (mm).

W: length of transverse member (mm).

It has been shown that for flat member, the torsional resistance (R) gives a greater accuracy than the polar moment of inertia [3]; therefore the twist angle (θ) can be written as follow:

$$\theta = \frac{TL}{RG}$$

Using the common formula for angular twist:

$$\theta_L = \frac{T_L L}{G n_L R_L} \qquad and \qquad \theta_T = \frac{T_T W}{G n_T R_T} \qquad\qquad (11)$$

Where:

T_L & T_T : the applied torque at the longitudinal and transverse member (N.mm), respectively.

n_L & n_T : number of longitudinal and transverse members, respectively.

R_L & R_T : torsional resistance of longitudinal and transverse member (mm^4) , respectively.

In this work, the cross-sectional area of longitudinal and transverse members is same and has a square area (A= 2x2 mm^2).

The torsional resistance for this section will be [3]:

$R= R_L = R_T = 0.1406 a^4$

Substituting equation (11) in to (10) gives:

$$\frac{\Delta}{W} = \frac{T_L L}{G n_L R_L} \qquad and \qquad \frac{\Delta}{L}$$

$$= \frac{T_T W}{G n_T R_T} \qquad\qquad (12)$$

Then:

$$T_L = \frac{\Delta G n_L R_L}{LW} \qquad and \qquad T_T = \frac{\Delta G n_T R_T}{LW} \qquad\qquad (13)$$

Since the applied torque is:

$$T_L = P_L W \qquad and \qquad T_T = P_T L \qquad\qquad (14)$$

$$\therefore P_L = \frac{T_L}{W} \qquad and \qquad P_T = \frac{T_T}{L} \qquad\qquad (15)$$

Substituting Eq.(15) in Eq.(13) give:

$$P_L = \frac{\Delta G n_L R_L}{LW^2} \qquad and \qquad P_T = \frac{\Delta G n_T R_T}{WL^2}$$

Since the external force (F) applied at the corner of frame is the sum of these two forces:

$$F = P_L + P_T = \frac{\Delta G n_L R_L}{LW^2} + \frac{\Delta G n_T R_T}{WL^2} = \frac{\Delta G}{WL}\left(\frac{n_L R_L}{W} + \frac{n_T R_T}{L}\right) \qquad (16)$$

or,

$$\Delta = \frac{FWL}{G}\left(\frac{1}{\left(\frac{n_L R_L}{W} + \frac{n_T R_T}{L}\right)}\right) \qquad (17)$$

Eq.(17) represents the theoretical vertical deflection of free end edge.

4. The Studied Cases

The deflection of free end for the frame sample shown in figure (4) is considered as a reference deflection under the applied load (F=1N) as compared with the other suggested frames.

The above frame consists of four rods (two in the longitudinal direction) have a length (L=200 mm) and (two in the transverse direction) have a length (W=100 mm). Each rod has a square cross-sectional area (A= 4 mm^2).

In order to reduce the deflection under the applied load and reinforce the frame, it was suggested to add three numbers of rods with the same cross-sectional area (A= 4 mm^2) to the above original frame as follows, table (1):

This table consists of adding only one rod to the original frame with four distributions (specimens group 1-4, set A), adding two rods to the original frame (specimens group 5-12, set B) and adding three rods to the original frame (specimens group 13- 28, set C).

The coordinates (x & y) and the inclined angels (θ & β) are listed in table (2).

5. ANSYS Procedure

The deflection of frame is analyzed with finite element method using (ANSYS 11). The following steps are done:

- Define the element type (ET: shell 181). This element is suitable for analyzing thin structures. It is a 4-node element with six degrees of freedom at each node; translations in the x, y, and z directions, and rotations about the x, y, and z-axes. This element is well-suited for linear, large rotation, and/or large strain nonlinear applications.
- Define the real constant for the above element (shell thickness = 2 mm).
- Define the material property with linear isotropic structure model (E=200 GPa, *v*=0.3).
- Molding area (drawing the frame).
- Meshing the specimen with fine free mesh.
- Applying the boundary conditions (two opposite edges simply supported and other free).
- Applying the concentrated force at the free ends (F=1N).
- Solve the current model and
- Plot the results of deflection for each specimen.

Table (1) All Samples of Case Studied

Table (2) The coordinates (x & y) and the inclined angels (θ & β)

No.	*Coordinate*	*No.*	*Coordinate*
1	x= 2, 5, 10, 15, 20, 30, 40, 50, 60, 70, 80, 90, 99 and 101 mm.	15	x=69 mm & θ=63.5^o
2	y= 5, 10, 15, 20, 25, 30, 35, 40, 45 and 49 mm.	16	x=69 mm & β=63.5^o
3	θ= 10, 20, 30, 40, 50, 60, 63.5, 70 and 80°	17	y=30 mm
4	β= 10, 20, 30, 40, 50, 60, 63.5, 70 and 80°	18	y=30 mm & x=101 mm.
5	x=101 mm & y=49	19	y=30 mm & θ=63.5^o
6	x=101 mm & θ=63.5^o	20	y=30 mm & β=63.5^o
7	x=101 mm & β=63.5^o	21	x=101 mm, y=49 mm & θ=63.5^o
8	y=49 mm & β =63.5^o	22	x=101 mm, y=49 mm & β=63.5^o
9	y=49 mm & θ =63.5^o	23	x=101 mm, θ=63.5^o & β=63.5^o
10	β =63.5^o & θ=63.5^o	24	y=101 mm, θ=63.5^o & β=63.5^o
11	x= 2,5,10,15,20,30,40,50,60,70,80,90 &99	25	x=101 mm & θ=26°
12	y= 5,10,15,20,25,30,35,40 &45	26	x=101 mm & θ=26°
13	x=67 mm	27	y=101 mm & θ=13.5^o
14	x=67 mm & y=49 mm	28	y=101 mm & θ=13.5^o

6. Results

The results include the deflection of free end under the applied load for each sample mentioned in table (1).

The deflection of basic frame shape (reference sample) shown in figure (4) is calculated using three methods; theoretical analysis, finite element method using MATLAP program and the ANSYS software program. Hence, the exact solution   (Eq. 17) is (1.93 mm.) which is close to the other methods with small error. Table (3) describes the results for three methods.

Table (3) deflection of basic frame shape

	Theoretical	*FEM*	*ANSYS*
Deflection (mm)	1.93	1.98	1.99

The other results of samples mentioned in table (1) have been calculated by two methods, finite element method using MATLAP program and the ANSYS software program. The behavior of deflection for samples (1, 2, 3, 4, 11 and 12) in table (1 &2) is shown in figures (6, 7, 8, 9, 10 & 11), respectively.
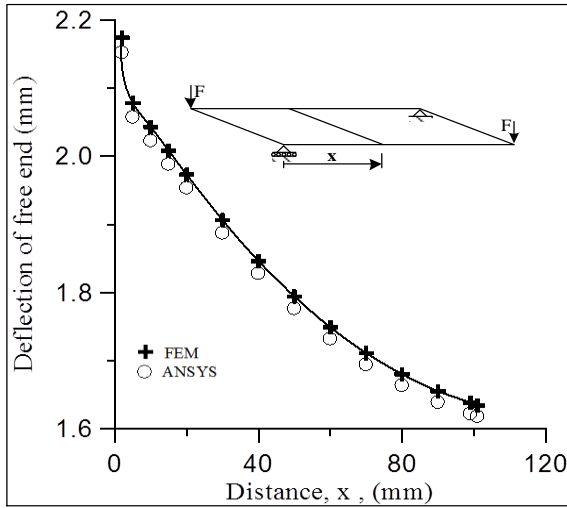
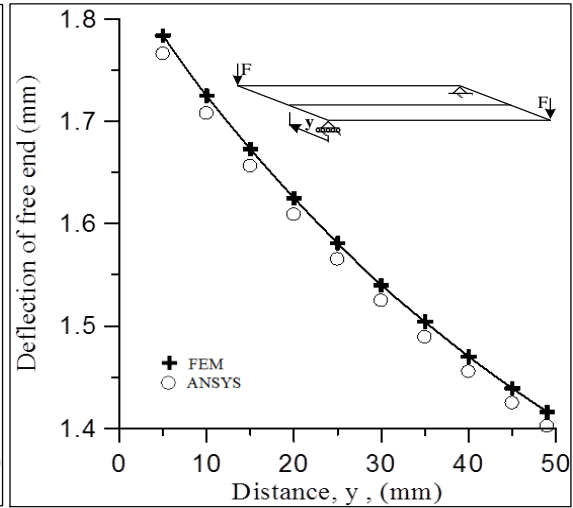Figure (6) Variation of free end deflection
with, x, for sample 1

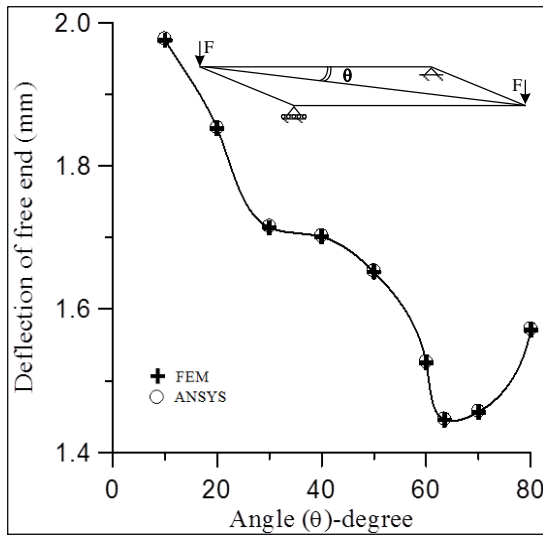Figure (7) Variation of free end deflection
with, y, for sample 2

Figure (8) Variation of free end deflection
with, θ, for sample 3

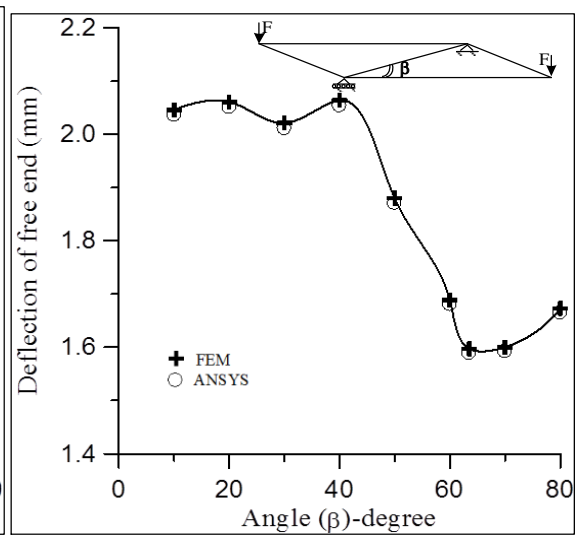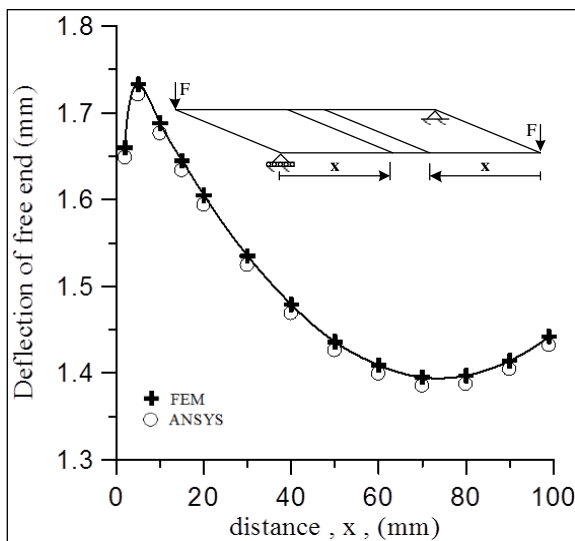Figure (9) Variation of free end deflection
with, β for sample 4

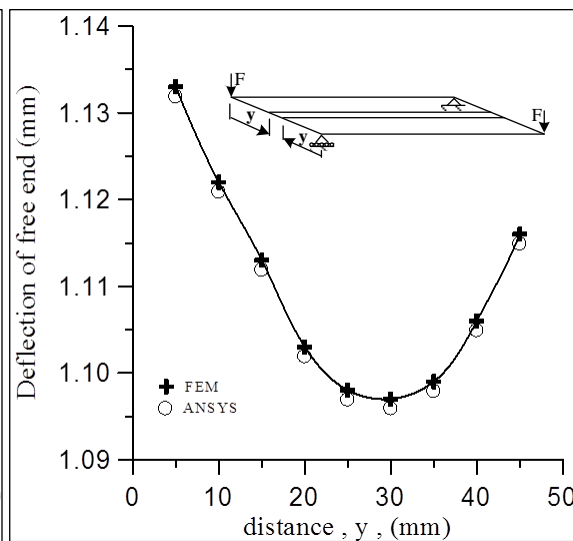Figure (10) Variation of free end deflection
with, x, for sample 11

Figure (11) Variation of free end deflection
with, y, for sample 12

In order to compare the deflection of all samples, the minimum deflection for each of the above samples and the other samples from table (1) is plotted in figure (12). Also, a simple result from the ANSYS program are shown in figures (13-18) which represents the deformed frame of some samples in set (B & C). As it is observed, the deflection of free end appears slightly resulted from the applied load.
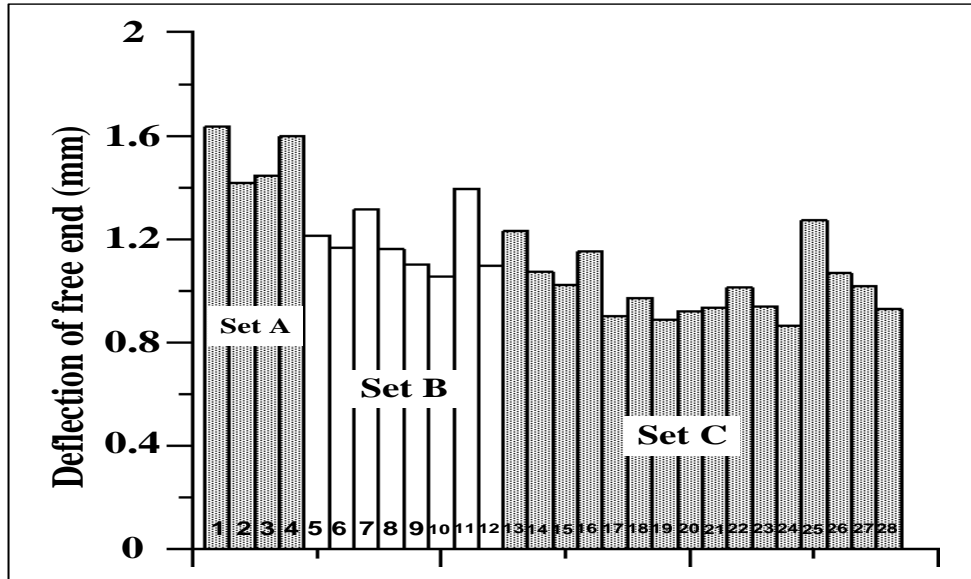

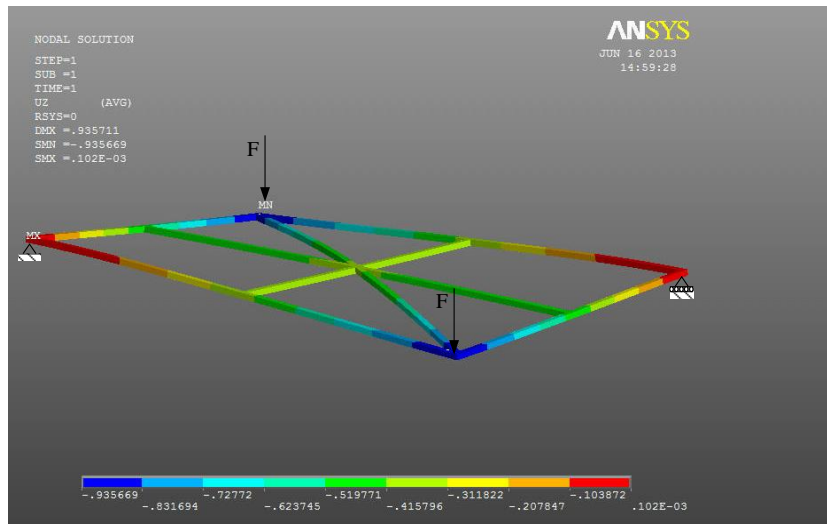Figure (12) The deflection of free end samples for all sets (A, B and C)

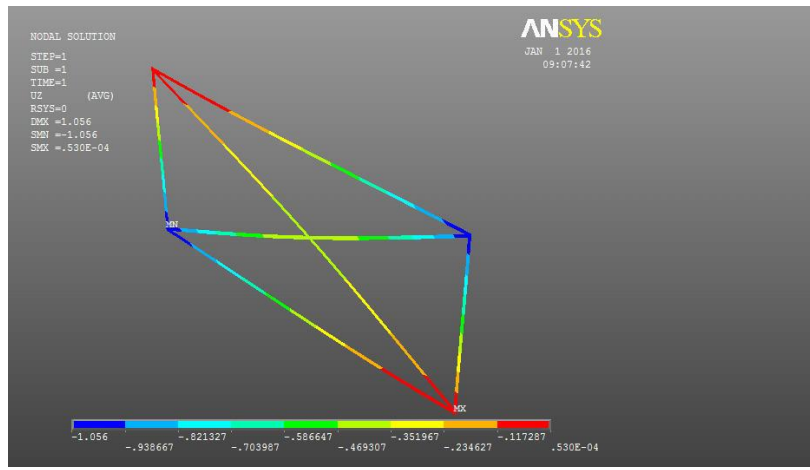Figure (13) The deformed shape of sample (21) in set (C)

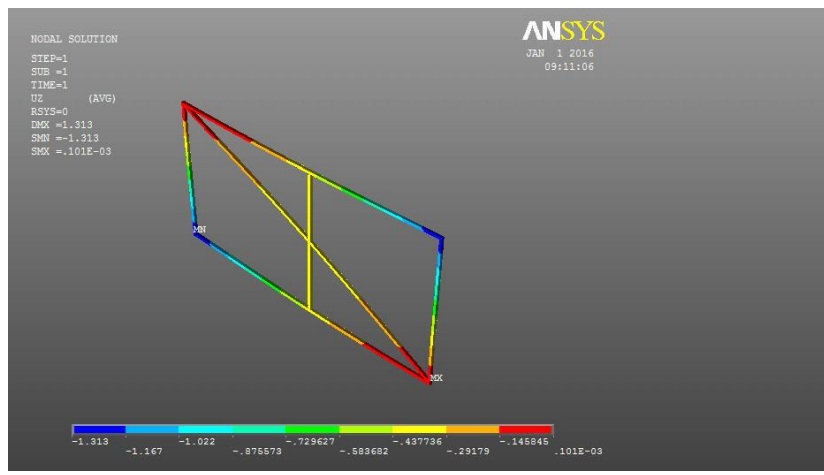Figure (14) The deformed shape of sample (10) in set (B)

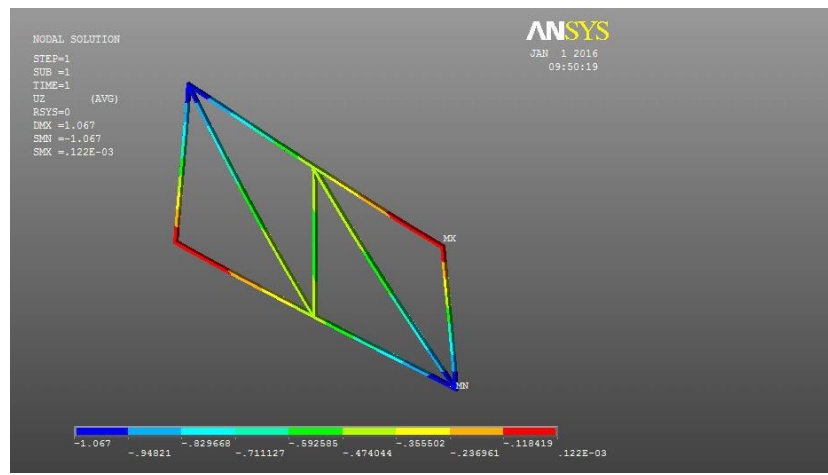Figure (15) The deformed shape of sample (7) in set (B)

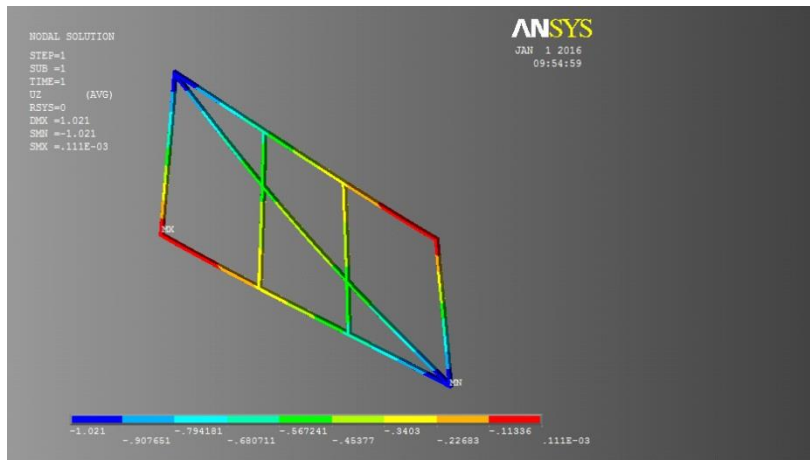Figure (16) The deformed shape of sample (26) in set (C)

70

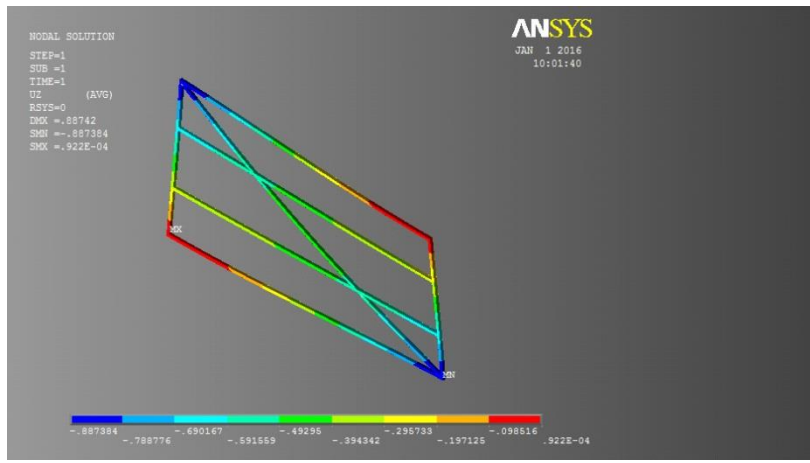Figure (17) The deformed shape of sample (15) in set (C)

Figure (18) The deformed shape of sample (19) in set (C)

7. Design of Experiment (DOE)

Design of experiment was used to assess the input factors and interactions that are important to the response. In a series of designed experiments, where the number of experimental runs are optimized, the important factors and interactions are identified. It can then look at optimizing the significant input settings in order to achieve the desired output [13 &14].
The designed matrix used in the fractional DOE consists of the following:
   (1) Input variables
   (2) Response
A Minitab program was used to input and analyze the data [15]. For input variables, coded units are used. Where, (+1) represents the existence the variable and (-1) represents the privation of variable.
The following table (4) defines the input variables used in Minitab program.

Table (4) The input variable in Minitab program

Variable	Definition (from table 1)
X1	One rod as in set(A), No1 with (x=101 mm)

X2	Two rods as in set(B), No11 with (x= 66.66mm)
X4	Three rods as in set(C), No13 with (x= 66.66mm)
Y1	One rod as in set(A), No2 with (y=49 mm)
Y2	Two rods as in set(B), No12 with (y= 33.33mm)
Y3	Three rods as in set(C), No17 with (y=33.33 mm)
T	One rod as in set(A), No3 with (θ= 63.5deg.)
B	One rod as in set(A), No4 with (β=63.5 deg.)
V	One rod as in set(C), No26 with (θ= 45deg.)
W	One rod as in set(C), No27 with (θ= 26.5 deg.)

All cases shown in table (1) have been studied according to the designed table (4). It is supposed that the deflection and cost of stiffeners of frame are the responses in Minitab program. The main target is to minimize the deflection and cost at the same time. The first response is deflection; hence, all the calculated deflections in each case were taken in the project window of Minitab. The second response is cost. It is assumed that the cost for each (100 mm stiffener length) is (1 unit). And hence, the cost of each stiffener length can be calculated.

Analyzing the experiments includes determination the factors that affect the responses and the significant interactions.

7.1. The Pareto Chart of the Standardized Effects:

The Pareto chart that is generated shows the significance of the terms. If any of the bars representing the terms go beyond the red line, they are significant. Figure (19) shows the Pareto chart for the first response (deflection). There are no more three way interactions. Most of the two way interactions are not significant which will be removed from this chart. The main factors are shown as significant as in fig.(20). As it has been observed, the main variable that effect on the deflection behavior is (T= θ).

The Pareto chart for cost illustrates lack of interactions, fig.(21). The maximum and minimum effect appears in variables (B & X2), respectively.
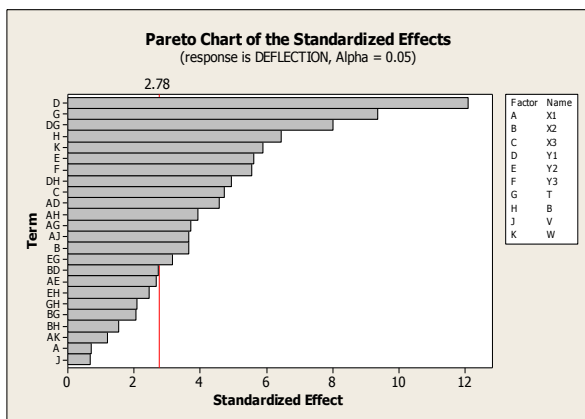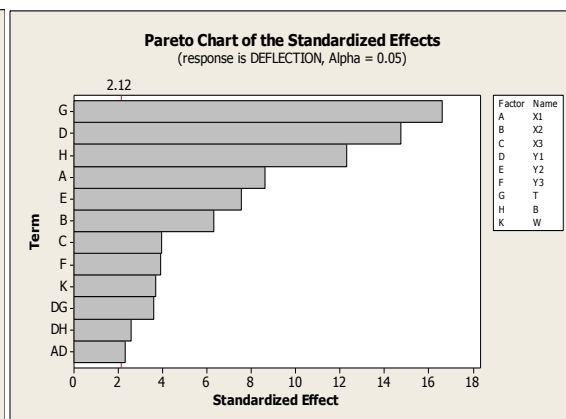

Fig.(19) Deflection Pareto chart   Fig.(20) Deflection Pareto chart (reviser)
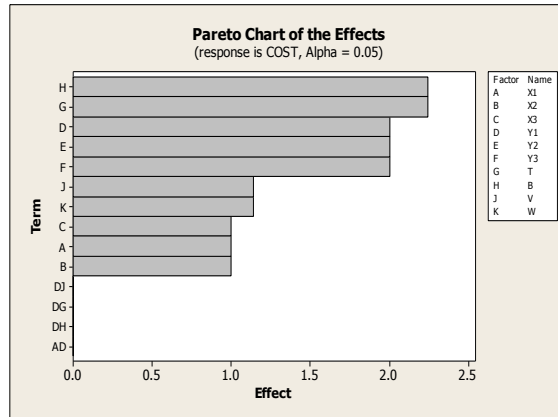
Fig.(21) Cost Pareto chart

7.2. *Main effect plot:*

The main target is to minimize the deflection by stiffener. This can be clarified from fig. (22). The Y-axis units are the same, therefore; the main effect that has the steepest line has the greatest effect on the deflection response. Approximately, the existence of variables (X1 & X2) has a diminish effect. The deflection reduced highly with the existence of variables (Y1,Y2 & Y3) . This effect being minimal with the existence. The main effect plot for cost, fig. (23) illustrates that the reduction in cost occurs in the existence of variables (X1, X2 & X3). On the other hand, the cost increases with the other variables.
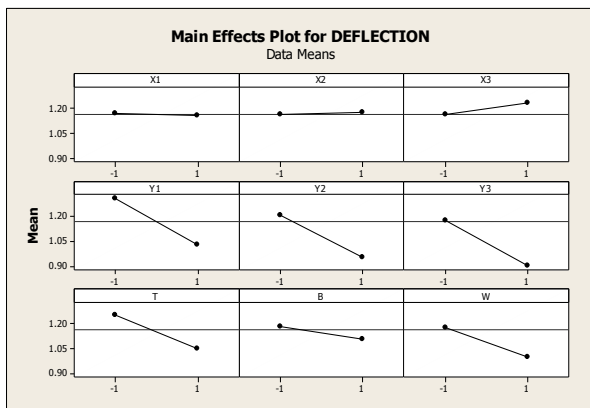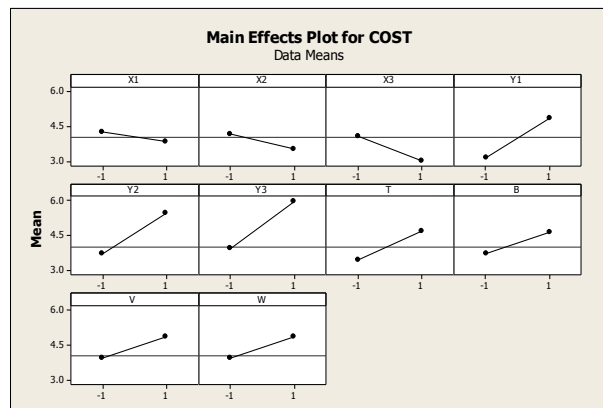

Fig.(22) Main effect plot for deflection

Fig.(23) Main effect plot for cost

7.3. *Interaction Plot for Deflection:*

The interaction induced between the variables (X1, Y1, T & B) is shown in fig. (24). The greater impact of the interaction variables occurs between (X1 & Y1). This interaction gives a higher reduction in deflection. The interaction between the other variables is significant, and it can be seen that the lines appear to be close to parallel.

In the response optimizer, the deflection can be found with minimum cost. The deflection is minimized to (0.8644 mm) with a minimum cost (5 unit). This can be occurred with the existence of the variable (X1, X2, X3, Y1) and the lack of other variables, fig. (25). This optimization has been achieved with importance (1 for deflection and 2 for cost).
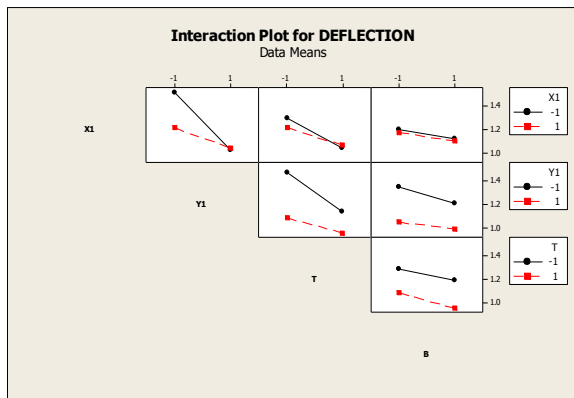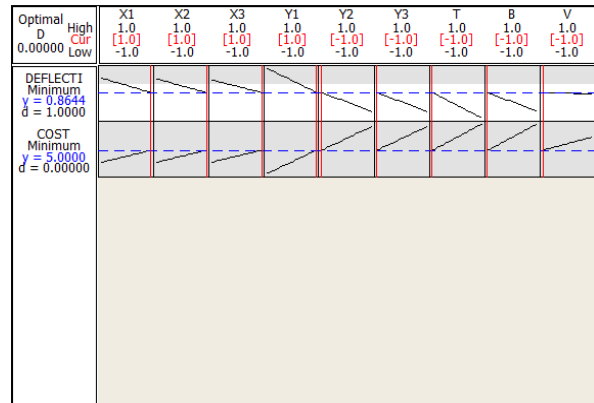
Fig.(24) Interaction plot for deflection

Fig.(25) Response optimizer

8. Discussion

Initially, a good accuracy is found as comparing the results of free end deflection between the ANSYS software and the FEM for all samples.

The deflection is decreased gradually as increasing the distance (x) in figure (6). Where, the deflection is reduced by ($\sim$ 18%) as compared with the reference sample. That means, the torsional resistance of the global frame depends on the distance (x). The greatest stiffness of this sample is found when the value of (x) is at the center of frame.

The torsional resistance for each bar depends on the type and dimension of its cross-sectional area. The cross-sectional area is constant for each bar. The increasing in the global resistance of frame depends on the torsional resistance for each bar as well as the location of the added or stiffened bar.

The same behavior is found in sample (2), figure (7). The deflection reduction for this sample is ($\sim$ 29%) when the location of (y) is at the center of frame.

For the inclined stiffened bar, sample (3), fig.(8), the deflection decreased with a non-uniform behavior. This is due to the non-uniform variation of global frame torsional resistance during increasing the angle (θ). The same behavior is found in the stiffened frame with angle (β), figure (9). The minimum deflection (maximum global torsional resistance) is found when the value of (θ & β = 63.5^o). This value occurred when the stiffened bar attached the corners of frame. A good distribution is found in the stiffened frame with angle (θ) as compared with that of angle (β).

Hence, the maximum deflection reduction for the first distribution is ($\sim$ 28%) and for the other distribution is ($\sim$ 20%). This means that the end stiffened bar connected at the edge of the applied load gives a good global frame torsional resistance as compare with the connection at the hinged edge.

On the other hand, increasing the number of stiffened bar results in increasing the global torsional resistance of the frame, figures (10 & 11). In general, increasing the distances (x & y) in the previous figures gave a reduction in the deflection of free end edge. The reduction is observed until the distances (x or y) divide the length or width of frame, respectively in equal spans. After this, the deflection behavior increases.

As comparing with the reference sample, the deflection is reduced by ($\sim$ 30%) at the point of equal span, figure (10) and by ($\sim$ 45%) , figure (11).

It may be concluded that the optimum reduction in deflection can be obtained when the stiffener bar (or bars) divides the longitudinal or transverse length of frame into equal span. Or, when the bar ends is attached at the frame corner. Therefore, the other sample is tested according to the above conditions. Figure (12) represents the deflection for all samples.

For set B, the minimum deflection is observed in sample (10). In which, the stiffeners bar are arranged with a cross shape. On the other hand, the minimum global frame torsional resistance (maximum deflection) is observed in sample (11), in which the stiffener bars are arranged in the transverse direction with equal span.

For set C, the maximum global torsional resistance observed in sample (24). In which, the first two stiffener bars are arranged with (X-shape), and the third bar is situated in the longitudinal direction. The weakest case is observed in sample (25). In which, the first two stiffener bars are arranged with (V-shape), and the third bar is situated in the transverse direction.

9. Conclusions

1-The proposed finite element model gave a good agreement when compared with the theoretical and ANSYS results.

2- A uniform reduction in the global torsional resistance is found when the stiffened bars are attached in the longitudinal and transverse direction.

3-The global torsional resistance depends on the distances (x, y).

4- The maximum torsional resistance is found when the stiffened bar is located at the center of frame.

5- Longitudinal bars gave a higher deflection reduction percentage as compared with the transverse bar.

6- The cross shape of stiffeners bar gave a minimum deflection.

7- The minimum global frame torsional resistance is observed when the stiffener bars are arranged in the transverse direction with equal span.

8- Torsional stiffness of stiffened frame depends on the stiffener bars distribution.

9- The existence of the inclined bar with ($\theta= 63.5^{o}$) gave the main effect on the deflection of frame.

10- The existence of the inclined bar with ($\beta= 63.5^{o}$) gave the main effect on the cost.

11- The existence of the longitudinal bars gave a higher deflection reduction as compared with the transverse and inclined rods.

12- The cost reduction is found in the existence of the transverse bars only.

10. References

1. Omer, W. Blodgett,(1963) "Design of Weldments". The James F. Lincoln Arc Welding Foundation. Colombia.

2. Paul, A. Seaburg and Charles, J. Carter,(2003) "Torsional Analysis of Structure Steel Members", American Institute of Steel Construction .

3. Omer, W. Blodgett, (1991) "Design of Welded Structures", The James F. Lincoln Arc Welding Foundation. Colombia.

4. Zoltan Virag,(2004) "Optimum Design of Stiffened Plates for Different Loads and Shape of Ribs", Journal of Computational and Applied Mechanics, Vol. 5., No. 1 .

5. Wang, Jingfeng and Li, Guoqiang,(2008) "Simplified Beam Design for Semi-Rigid Composite Frames at the Serviceability Limit State", Tsinghua Science and Technology, Vol. 13, No. 5 .

6. David, A. Pape and Angela, J. Fox,(2006) "Deflection Solutions for Edge Stiffened Plates", Proceedings of The 2006 IJME - Intertech Conference.

7. David, V Hutton, (2004)"Fundamentals of Finite Element Analysis", Mc-Graw Hill.

8. Yu-Qiu, Long; Song Cen and Zhi-Fei Long,(2009) "Advanced Finite Element Method in Structural Engineering", Tsinghua University Press, Beijing and Springer-Verlag GmbH Berlin Heidelberg.

9. A. Kaveh,(2014) "Computational Structural Analysis and Finite Element Methods", Springer International Publishing Switzerland.

10. A, J. M. Ferreira,(2009) "MATLAB Codes for Finite Element Analysis", Springer Science & Business Media B.V. ,.

11. Young, W. Kwon and Hyochoong, Bang.,(2000) "The Finite Element Method using MATLAB". CRC Press LLC.,.

[12] Amar Khennane,(2013) "Introduction to Finite Element Analysis using MATLAB and Abaqus", Taylor & Francis Group, LLC.,.

13. Jiju Antony, "Design of Experiments for Engineers and Scientists", Elsevier Science & Technology Books, 2003.

14. Peter G.,(2013) "Optimal Design of Experiments A Case Study Approach", John Wiley & Sons, Ltd.,.

15. Rehman, M. Khan,(2013) "Problem Solving and Data Analysis using Minitab", John Wiley & Sons, Ltd,.